

**CALCULATION OF THE INFLUENCE
OF THE INJECTION RATE OF CARRIERS
ON THE VOLT-AMPERE CHARACTERISTICS
OF THE nc-Si/CaF₂ MULTILAYER STRUCTURE
BY THE METHOD OF PARALLEL CALCULATIONS**

V. A. Sizyuk,^a G. V. Miloshevskii,^b and
I. Yu. Smurov^c

UDC 621:382+519.6

On the basis of the Monte Carlo method a theoretical model of charge transfer processes in the multilayer nc-Si/CaF₂ structure has been developed. The constructed self-consistent model has made it possible to investigate the influence of the injection rate of charge carriers and the potential barrier height of a dielectric on the volt-ampere characteristic of the structure. The dependence of the rate of injection from a contact on the applied external voltage has been calculated. The main problem (large counting time) of the theoretical model has been solved by organizing parallel calculations in the developed code SIMPS. The realization of the SIMPS code written in the programming language Fortran-95 on a computer cluster for parallel calculations with distributed memory is presented. The results of the calculations demonstrate an increase in the calculation rate with increasing number of processors.

Introduction. The progress made in the advancement of equipment and technologies of microelectronics has led in the last few years to the creation of materials with the so-called "natural quantum confinement" (NQC). The quantum nature of the processes proceeding in nanodimensional structural units of these materials leads to a change in the electronic and optical properties of the whole system. As is known, the most widely used and the cheapest, to date, material of microelectronics — crystalline silicon — is unsuitable for constructing light-emitting devices because of the peculiarities of its band structure. The technology of depositing thin layers of equally oriented nanodimensional crystals of silicon (the so-called nanocrystalline silicon nc-Si) on CaF₂ substrates, which has been developed in the last two to three years [1, 2], has made it possible to obtain on its basis a direct-band semiconductor. Unlike the already well-known porous silicon, this technology provides much better reproducible results, which enables one to forecast the development of industrial semiconductor devices on its basis. One of the most promising directions of investigations in this connection is the use of the properties of the nc-Si band structure for constructing light-emitting devices.

Today a number of experimental works devoted to the investigation of electroluminescence in nanocrystalline silicon and its use for constructing light-emitting devices are known [1–3]. The authors note a strong influence of high potential barriers of the CaF₂ dielectric layers on the electrophysical and optical characteristics of the structure. As one variant of overcoming this difficulty, in [1] a structure in which the field is applied along the nc-Si/CaF₂ layers is proposed. The problem of injecting charge carriers into structures is mentioned in these works; however, it is given less consideration and, as is known, contact phenom-

^aA. V. Luikov Heat and Mass Transfer Institute, National Academy of Sciences of Belarus, Minsk, Belarus; email: sva@hmti.ac.by; ^bDepartment of Chemistry, Brandeis University, Waltham, Massachusetts, USA; email: miloshevsky@yahoo.com; ^cÉcole Nationale d'Ingénieurs de Saint-Etienne, France; email: smurov@imp-odeillo.fr. Translated from *Inzhenerno-Fizicheskii Zhurnal*, Vol. 75, No. 1, pp. 133–141, January–February, 2002. Original article submitted May 16, 2001.

ena produce a considerable effect on the processes in the structure and on the electrophysical properties of the device on the whole. The authors of the present paper investigate the influence of the injection rate of electrons from the A1-contact as well as the influence of the potential barrier height of dielectric layers on the volt-ampere characteristic of the multilayer nc-Si/CaF₂ structure on the basis of the results of the numerical experiment performed with the aid of the developed program code SIMPS.

In describing semiconductor structures, the Boltzmann equation can be solved directly only with considerable simplifications and asymptotic assumptions in the initial model. Therefore, for modeling charge-transfer processes in the nc-Si/CaF₂ periodic structure, we used the ensemble Monte Carlo method [4]. In solving a self-consistent problem, this method presupposes a large volume of calculations. This fact is now the main deterrent to wide application of the Monte Carlo method of calculations. For instance, to obtain one point on the volt-ampere curve of the structure being investigated, with regard for the anisotropic law of dispersion for holes in our formulation of the problem about 20 h of operation of a P-166 processor are needed. In the present paper, the problem of the large counting time is solved by organizing parallel calculations.

In the architecture of contemporary multiprocessor computers, two major directions are notable [5]: (a) symmetric multiprocessor systems SMP with a shared memory (RM 600 E, DEC AlphaServer 8200/8400, SGI POWER CHALLENGE); (b) MPP (Massively Parallel Processing) supercomputers with architecture with a physically and logically distributed random-access memory (Cray 73D, Cray T3E, SPP1200/XA, IBM RS/6000 SP2). An SMP computer comprises the shared memory file and a set of identical processors. In this architecture, they have equitable access to the whole space of random-access memory. The presence of the shared memory simplifies the interaction between the processors, but strongly limits their number. In such computers, the total number of processors usually does not exceed 32, since a further increase gives no advantage because of the conflicts in accessing the shared memory. From the point of view of the applied problem, the SMP computer is an integral system with computational resources proportional to the number of processes. The main advantage of SMP computers over MPP machines is the relative ease of programming. Many of the programs developed for one-processor computers in the programming languages Fortran and C⁺⁺ can be automatically paralleled by means of OpenMP translators [6]. At present, two- and four-processor Pentium- and Pentium Pro-based SMP computers functioning in the Windows NT medium are readily available.

The supercomputers developed by the MPP technology combine thousands of processors by linking each of them with the local memory due to the employment of a high-speed communication infrastructure. Each processor has access only to its own memory. Access to a remote memory is only possible with the use of a message-exchange system. All machines with a computing power of hundreds of billions of operations per second are based on this approach. MPP supercomputers are the most expensive and powerful computers in the world. One way to reduce the cost of MPP computers is the rejection of nonstandard communication equipment in favor of conventional network equipment. Such a supercomputer is a cluster consisting of several computers integrated by a high-speed network (Ethernet, FDDI, ATM, HiPPI, etc.). Clusters can be formed from both different and identical computers. Each computer in the cluster is autonomous with an individual operational system and its own system resources. Modern clusters have characteristics comparable in many ways to MPP supercomputers. If we add to this their relatively low cost, it becomes clear why these much cheaper (compared to MPP machines) computers have found wide application in the last few years. Unlike the SMP computers, a cluster as a system is formed at the applied level and not at the level of an operational system. Programming in such a medium is a rather difficult task and requires special software for the operation of parallel applications. The use of the programming language High Performance Fortran (HPF) for the model of message-exchange distributed memory is promising. However, HPF features, so far, a low efficiency as compared to the direct use of the message-exchange library MPI [7, 8].

Experimental Procedure and Basic Assumptions. The physical conditions of the experiment and the main geometrical and technological parameters of the multilayer structure are analogous to those presented in [9]. The comparison of the obtained numerical results with the experimental data was also made on

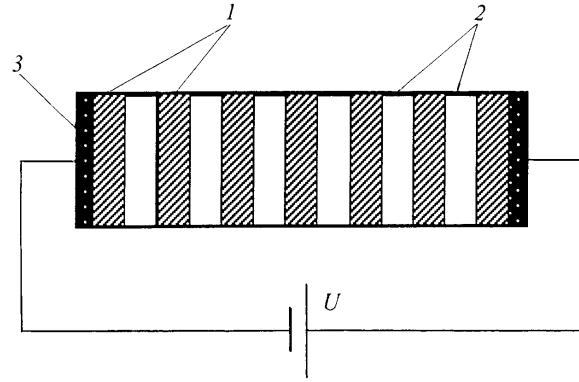


Fig. 1. Diagram of the device: 1) Si layers; 2) CaF₂ layers; 3) contacts.

the basis of the data of [9]. The structure under investigation is schematically represented in Fig. 1. The cathode and anode of the device comprise effective injectors of electrons (Al-contact) and holes (indium tin oxide contact). In the constructed model, a structure with quantum wells formed by alternating epitaxial layers of nanocrystalline silicon and calcium difluoride is considered. It takes into account the processes of electron-hole tunnel transitions between individual layers and the interaction of carriers with optical and acoustic oscillations of the nc-Si lattice, as well as the recombination at the boundaries of nanocrystals. From the point of view of this model, the interaction of electrons with optical oscillations of the lattice was thought to be small under the assumption of an isotropic parabolic conduction band [10].

Following the assumptions of [9], it is assumed that current transfer in the structure proceeds via elastic tunneling of electrons and holes through the dielectric layers and their drift in the semiconductor layers. The probability of tunneling was calculated in the Wentzel–Kramers–Brillouin (WKB) approximation [11]. A nondegenerate conductor was considered. As our investigations have shown, the electrical properties of the structure strongly depend on the distribution function of charged particles injected from contacts. This is primarily due to the small length of the device exceeding the mean free path of the charge carriers only a few times. The injection of particles into the device is also described in terms of the WKB approximation.

The self-consistent character of the electric fields is taken into account: the influence of the charge of particles of both signs injected from contacts on the electric field distribution in the device (curvature of the interlaminar energy barriers), screening by the charge of individual layers of the structure, and the reverse influence of the electric field on the charge distribution.

Physicomathematical Model. *Charge carrier transport.* The electric potential distribution φ in the structure was calculated by the tri-diagonal method [12] on a uniform grid $n = 0, \dots, N$ with a step h along the device axis

$$\frac{1}{h^2} \varphi_{n-1} - \frac{2}{h^2} \varphi_n + \frac{1}{h^2} \varphi_{n+1} = Q_n, \quad (1)$$

with boundary conditions of the first and fourth kind:

$$\varphi_0 = 0, \quad \varphi_N = U, \quad \varepsilon_n \left. \frac{d\varphi}{dx} \right|_- = \varepsilon_{n+1} \left. \frac{d\varphi}{dx} \right|_+.$$

For the involved case of the permittivity ε_n variable over the structure layers, the tri-diagonal coefficients are equal to

$$\alpha_{n+1} = \frac{\varepsilon_{n+1}}{\varepsilon_n + \varepsilon_{n+1} - \varepsilon_n \alpha_n}, \quad \beta_{n+1} = \frac{\varepsilon_n (\beta_n - Q_n h^2)}{\varepsilon_n + \varepsilon_{n+1} - \varepsilon_n \alpha_n}. \quad (2)$$

To satisfy the Poisson equation, the method of "macroparticles" [4] is used in the present work. But the utilization of macroparticles leads to the need for rather small time steps for the procedure to converge. Because of this fact we had to abandon the introduction of "fictive" scattering [13] in drawing the time of the

particle free path in favor of numerical integration of the equation $\int_0^\tau W_{\Sigma}(\mathcal{E}) dt = -\ln r$ by means of simple summation on each time layer. When the integral on the left side of this equation that has accumulated during the time of particle free flight exceeds the random value given at the start of the cycle, the scattering is drawn according to the probability curves. After the scattering a new random value of $-\ln r$ is given. Upon the expiration of the time step the field in the structure is recalculated and the procedure is repeated.

The equations of motion for electrons under the assumption of an isotropic parabolic conduction band have a classical form and are considered in detail in [10]. Taking into account the considerable anisotropy of the valence band of the form $\mathcal{E}(\mathbf{k}) = ak^2[1 - g(\vartheta, \psi)]$ leads to a complication of the equations of motion for holes and the necessity of calculating the integrals in time t :

$$x = -\frac{Ap_{0x}}{m_{el}} \int_0^t g dt + \frac{Ap_{0x}}{m_{el}} t + x_0, \quad y = -\frac{Ap_{0y}}{m_{el}} \int_0^t g dt + \frac{Ap_{0y}}{m_{el}} t + y_0, \quad (3)$$

$$z = -\frac{AeE}{m_{el}} \int_0^t t g dt - \frac{Ap_{0z}}{m_{el}} \int_0^t g dt + \frac{eAEt^2}{2m_{el}} + \frac{Ap_{0z}}{m_{el}} t + z_0,$$

where $g(\vartheta, \psi) = \sqrt{b^2 + c^2(\sin^4 \vartheta \cos^2 \psi \sin^2 \psi + \sin^2 \vartheta \cos^2 \psi)}$ depends on the azimuth ψ and radial ϑ angles of motion of a hole. Here $a = \frac{\hbar^2 |A|}{2m_{el}}$, $b = \frac{|B|}{|A|}$, and $c = \frac{|C|}{|A|}$.

The tunneling of charge carriers via the potential barriers of CaF_2 layers and the potential barriers of contacts is described in terms of the WKB approximation and parabolic approximation of the form of potential barriers [11]. The action of the force of mirror reflection leads to a decrease in the potential barrier width and height as a result of the smoothing of its angles. For the force potential of the mirror reflection the authors used the expression

$$\Phi_1(x) = -\frac{e^2}{4\pi\varepsilon} \left\{ \frac{1}{2x} + \sum_{n=1}^{\infty} \left[\frac{nS}{(nS)^2 - x^2} - \frac{1}{nS} \right] \right\}. \quad (4)$$

The charge transfer in tunneling via the CaF_2 potential barriers was realized with the use of the statistical weight method of [10] modified by the authors. At the start of the code it was assumed that the probability of overcoming the potential barrier in the direction of the field for the particles is 0.95 and counter to the field — $1.0 \cdot 10^{-5}$, and in accordance with these probabilities the tunneling for particles was drawn. The true (calculated) values of the probability that the charge carriers have passed the barrier were taken into account by the change in their statistical weight.

The calculation of the energy parameters of the initial electron and hole beams in terms of the WKB approximation was carried out in accordance with the technique developed by the authors and described in more detail in [14].

Carrier scattering. In describing the motion of charge carriers inside the Si-grains, the interactions with the acoustic and optical oscillations of the semiconductor lattice were taken into account. By virtue of the fact that nanocrystalline silicon practically becomes a direct-gap semiconductor [15] the scattering of conductivity electrons is described in terms of the isotropic parabolic dispersion law. According to this, the expression for the probability of absorption or emission of acoustic phonons by electrons takes on the form [10]

$$W_{\text{ac}}^{\pm}(k) = \frac{\Xi_{\text{ac}}^2 m_{\text{el}}^*}{4\pi\rho s_{\text{long}} \hbar} \frac{1}{\hbar k} \int_{q_{\text{min}}^{\pm}}^{q_{\text{max}}^{\pm}} \left(N_{\text{ac}} + \frac{1}{2} \pm \frac{1}{2} \right) q^2 dq, \quad (5)$$

$$q_{\text{min}}^+ = \begin{cases} 2[q_s - k], & k < q_s; \\ 0, & k \geq q_s; \end{cases} \quad q_{\text{min}}^- = 0; \quad q_{\text{max}}^+ = 2[q_s + k]; \quad q_{\text{max}}^- = \begin{cases} 0, & k \leq q_s; \\ 2[q_s - k], & k > q_s; \end{cases}$$

$$q_s = \frac{m_{\text{el}}^* s_{\text{long}}}{\hbar}.$$

For the valence band, taking into account the anisotropy leads to the expression [16]

$$W_{\text{ac}}^{\pm}(\mathcal{E}) = \frac{\Xi_{\text{ac}}^2 m_{\text{hh}}^{*1/2} (k_{\text{B}}T)}{2^{9/2} \pi \rho s_{\text{long}} \hbar^4 \mathcal{E}^{1/2}} (F^{\pm} + (k_{\text{B}}T/\mathcal{E}) G^{\pm}), \quad (6)$$

where

$$F^{\pm}(x) = \int_0^{x\sqrt{2}} z^2 \left(1 + 3(1 - z^2/x^2)^2 \right) \left[N(z) + \frac{1}{2} \mp \frac{1}{2} \right] dz,$$

$$G^{\pm}(x) = \int_0^{x\sqrt{2}} z^3 \left(1 + 3(1 - z^2/x^2)^2 \right) \left[N(z) + \frac{1}{2} \mp \frac{1}{2} \right] dz,$$

at

$$x = 2 \sqrt{m_{\text{hh}}^* s_{\text{long}}^2 \mathcal{E} / k_{\text{B}}T}.$$

Only the "heavy" holes were taken into account since the contribution of the "light" holes is small because of the low density of states in the valence band [17]. The maximum value for the probability density of the energy distribution of acoustic phonons for them

$$P^{\pm} = (1 + 3 \cos^2 \theta) \frac{\{(1 - \cos \theta) (\mathcal{E}(k) \pm \mathcal{E}_q)\}^{1/2}}{\{a [1 - g(\vartheta', \psi')]\}^{3/2}} \frac{1}{\exp(\hbar s_{\text{long}} q / k_{\text{B}}T) - 1} + \frac{1}{2} \mp \frac{1}{2} \quad (7)$$

was chosen on the basis of the energy value $\mathcal{E}_q = \hbar s_{\text{long}} q$ of the acoustic phonon equal to $10^{-2} k_B T$. As the minimum energy of the acoustic phonon, the authors used values up to $10^{-4} k_B T$, but this did not lead to changes in the results of the numerical experiment because of the small probability of such events and the small displacement of particles caused by it. The above assumption led to the possibility of using the Neumann procedure [10] for drawing the final state of the holes after their interaction with the acoustic phonons.

Since the effective mass of the density of states in the valence band practically coincides with the averaged effective mass of the carriers [16], the expression for the probability of interaction between the holes and the deformation potential of the optical phonons in accordance with the anisotropic law of dispersion coincides with the expression for the probability of interaction in the isotropic case:

$$W_{\text{op}}^{\pm}(\mathcal{E}) = \frac{\Xi_{\text{op}}^2 m_d^{*3/2}}{\sqrt{2} \pi \rho \hbar^3 \omega_{\text{op}}} \left(N_{\text{op}} + \frac{1}{2} \mp \frac{1}{2} \right) \sqrt{\mathcal{E} \pm \hbar \omega_{\text{op}}} \Theta(\mathcal{E} \pm \hbar \omega_{\text{op}}), \quad \Theta(x) = \begin{cases} 1 & \text{for } x > 0, \\ 0 & \text{for } x < 0. \end{cases} \quad (8)$$

The anisotropy was taken into account by drawing the final direction angles of the hole in accordance with the probability density distribution $P_{\text{op}} = 1/[1 - g(\vartheta, \psi)]^{3/2}$ with the use of the Neumann procedure.

Modeling of recombination processes was carried out according to the theory of [17]. In so doing, it is assumed that the charge-carrier recombination occurs at the boundaries of nanocrystals where the luminescence centers are situated. Two types of processes were considered: (a) electron capture to the free level with photon emission and annihilation of the hole on the photon; the transition is characterized by the concentration of all the levels at the boundaries of nanocrystals, the concentration of the free levels, and the electron energy; (b) transition of the electron from the boundary level to the valence band (hole ionization); the process is also characterized by the total concentration of the levels and the concentration of occupied levels and proceeds by the nonradiative mechanism.

Realization of the SIMPS code on parallel processors. For carrying out parallel calculations, in the laboratory of radiation gas dynamics of the Academic Scientific Complex of the A. V. Luikov Heat and Mass Transfer Institute of the National Academy of Sciences of Belarus an NT-MPICH program package of paralleling on five IBM PC computers with Intel processors linked by a local network with a TCP/IP protocol was installed. In this cluster system, to organize an interaction between processes being executed on different computers in solving the same problem, the MPI message exchange model is used. With the aid of the NT-MPICH package we familiarized ourselves with the software of the MPI library and adapted the program complex SIMPS for parallel calculations controlled by the Windows NT 4.0 operating system. The MPI is now the most widely used model of parallel programming. On initiating the SIMPS the MPI message-exchange system separates a fixed number of identical processes and does not allow these subprograms to be created or destroyed during the program execution. Each process is identified by a unique name and is executed on one of the processors. Initially all subprograms are in the nonexecution state except for process 0, which is executed off-line until a parallel construction is encountered in it. Then, by means of calling procedures from the MPI library, it activates the inactive processes. All subproblems are run independently unless they are explicitly coordinated by means of waiting for messages. Not a single process can access the variables of its neighbor. At the end of a parallel construction the subproblems coordinate their mutual operations and share the data values by means of explicit transfer of messages. This enables individual processes to remain weakly synchronized and thus achieve a good speeding-up due to the strong parallelism and also enables them to carry out direct exchanges without calling the operating system, which leads to an increase in the performance.

For creating the SIMPS code to be executed, the Compaq Visual Fortran 6.1a program package was used. Execution was started by the RexecShell shell [18], which permitted creation, control, and check of the processes. To ensure the computer cluster functioning in the Windows NT operating medium, the NT Cluster

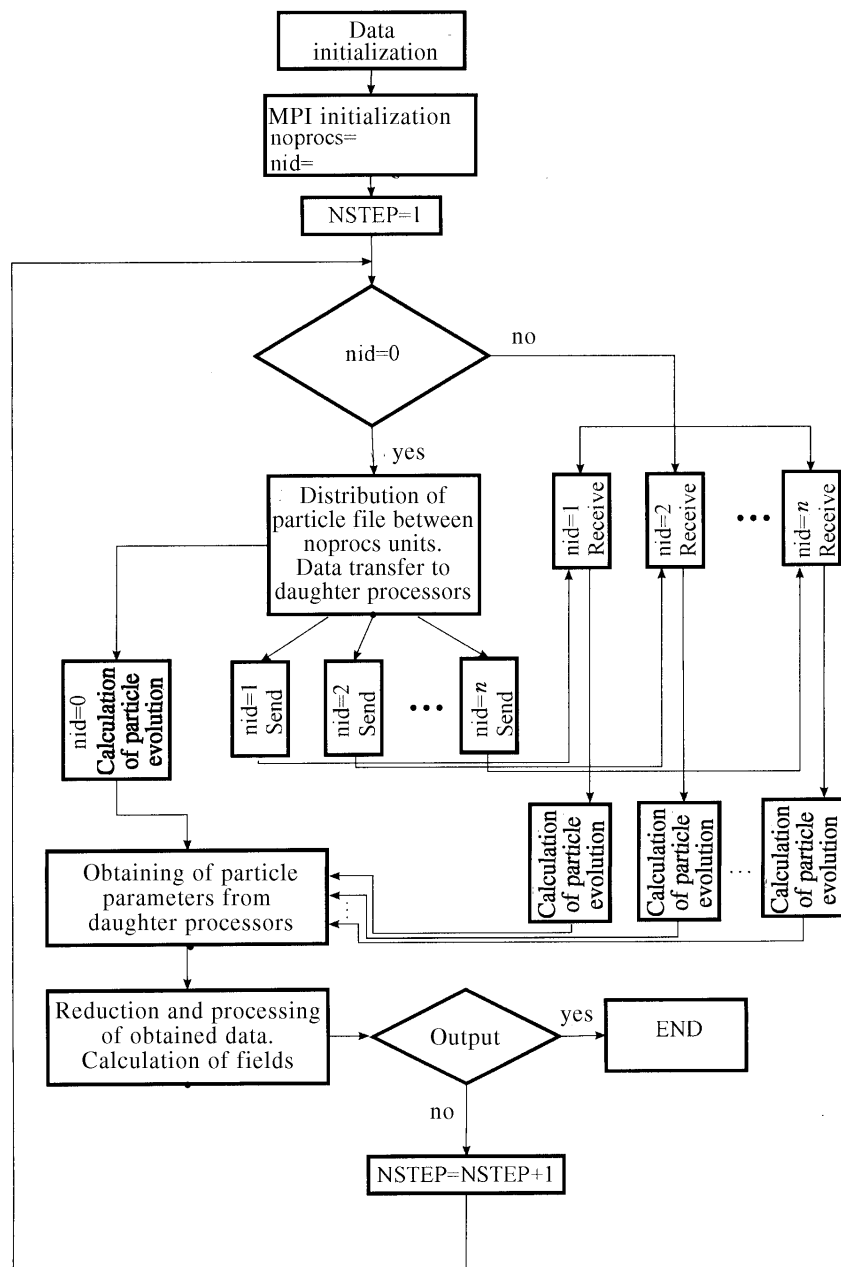


Fig. 2. SIMPS code paralleling algorithm

Manager (cluma) service was used. This service made it possible to provide communication and control of the processes in the cluster. In the general case, some of the cluster nodes are configured as computational and are used for starting user jobs. The other nodes have certain resources (local memory, disk space), offering various services needed for executing jobs. When a parallel job enters the cluster system, the RexecShell shell requests the required number of nodes. The system aids allocate to this job the required nodes and the job initiates the operation. The cluster permits concurrent operation of several parallel jobs started from different computational nodes, each of which is executed on a certain set of processors.

Because of the relative complexity of parallel computers and their great difference from single-processor machines, one cannot simply make use of the traditional programming languages and expect a good performance. Therefore, the problem of program paralleling becomes first and foremost. The algorithm for modeling the charge transfer in a three-dimensional dielectric-semiconductor periodic structure is based on the

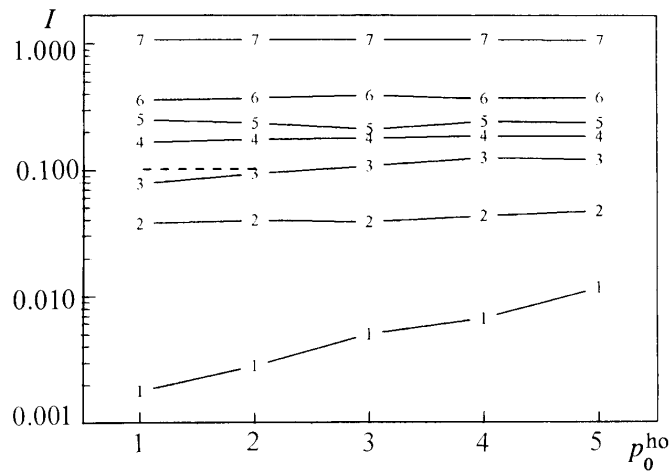


Fig. 3. Dependence of current I in the nc-Si/CaF₂ structure on the initial pulse of injected carriers at $U = 5$ V. Electron momentum: 1) $0.8 \cdot 10^{-20}$ g-cm/sec, 2) $2.0 \cdot 10^{-20}$, 3) $2.3 \cdot 10^{-20}$, 4) $2.5 \cdot 10^{-20}$, 5) $2.5 \cdot 10^{-20}$, 6) $2.8 \cdot 10^{-20}$, and 7) $3.5 \cdot 10^{-20}$; dashed curve — current level in the experimental structure [9]. I , mA; p_0^{ho} , 10^{-21} g-cm/sec.

use of the Monte Carlo ensemble method. Since the kernel of the Monte Carlo method in general and of the given complex in particular consists of statistical data accumulation, SIMPS admits splitting into several equitable processes. Paralleling presents an additional difficulty, since it calls for controlling the operation of the processors and coordinating the interprocessor interactions. The paralleling scheme is presented in Fig. 2. The code provides for initial initialization of a certain common file of particle parameters, calculation of the electric field distribution in the structure, and calculation of the change in the particle parameters in one time step. Calculations of the electric field and evolution of particles per time step alternate until equilibrium is attained. To solve this problem on a parallel computer, it is necessary to distribute the calculations between the processors so that each processor runs a part of the problem. At the start of the algorithm, in initializing the MPI, the code finds the total number of linked processors n_{procs} and assigns to each of them its identification number n_{id} . For the master processor the identifier n_{id} is 0. In realizing the SIMPS complex on parallel computers, the common file of particle parameters is broken up into units (according to identifiers n_{id} , see Fig. 2), each of which is accessible to only one individual processor. Thus, each computer node will be calculating the evolution of not the common file of particles but only of a part of it. At the end of a time step each node sends a message about new parameters of particles to the master processor. This processor calculates the electric field, which has changed because of the redistribution of particles, for the whole file and transfers these data to the other nodes. Thus, the medium of parallel programming NT-MPICH ensures adequate control of the distribution of calculations and data communications.

Results. Using the above-described model and methods, we managed to obtain the volt-ampere characteristics of the nc-Si/CaF₂ structure for various conditions without resorting to the direct solution of the Boltzmann kinetic equation. We investigated the influence of the rate of charge carrier injection from contacts on the total current of the device. As the numerical calculation has shown, the electron injection rate produces a noticeably greater effect on the volt-ampere characteristic of the instrument than the hole injection rate at a rated concentration of carriers in the beam of $1.0 \cdot 10^{11}$ cm⁻³ (Fig. 3). First of all, this is due to the fact that, as follows from the model, electrons are the main current carriers in the structure under consideration. On the assumption of direct tunneling through the potential barrier of the dielectric the passage probability for electrons appears, on average, to be higher than for holes. As seen from Fig. 3, an increase in the initial pulse of electrons by $0.5 \cdot 10^{-20}$ g-cm/sec leads to a change in the current at least by a factor of two,

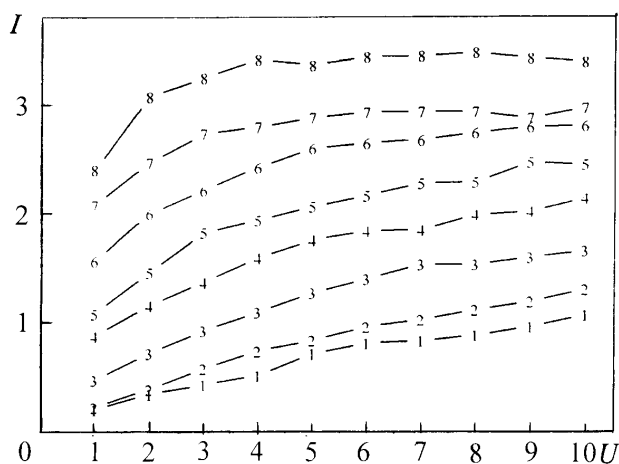


Fig. 4. Volt-ampere dependences of the periodic nc-Si/CaF₂ structure at a dielectric potential barrier height for electrons and holes, respectively: 1) 0.5 eV, 0.4 eV; 2) 0.5 and 0.3; 3) 0.4 and 0.3; 4) 0.3 and 0.3; 5) 0.3 and 0.2; 6) 0.2 and 0.2; 7) 0.1 and 0.2; 8) 0.1 and 0.1. I , mA; U , V.

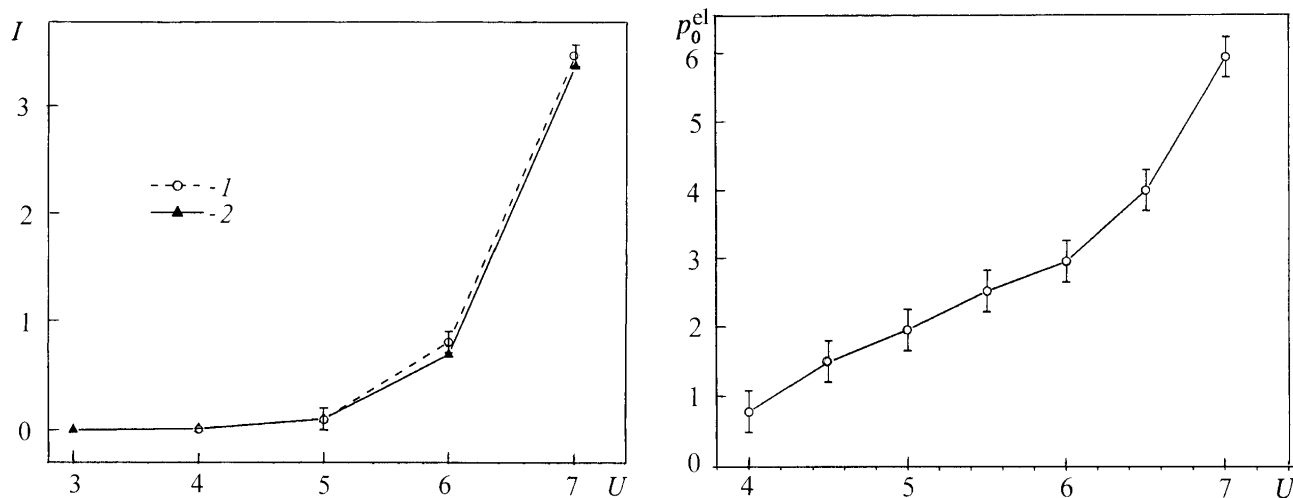


Fig. 5. Calculated (1) and experimental (2) [9] volt-ampere dependences on the assumption of an infinitesimally small hole component of the current at a CaF₂ potential barrier height of 0.5 eV. I , mA; U , V.

Fig. 6. Calculated dependence of the initial pulse of electrons injected from a contact into the nc-Si/CaF₂ structure. p_0^{el} , 10^{-20} g·cm/sec; U , V.

whereas for holes departures of current are noticeable only at very low injection rates of electrons. For orientation, the dashed line in the figure shows also the current level in the real structure with calculated geometrical sizes and an external voltage of 5 V from the experimental work of [9]. The curves depicted in Fig. 3 were calculated on the assumption of effective potential barriers of CaF₂ layers of 0.5 eV for electrons and 0.4 eV for holes. At higher barriers the tunnel current rapidly drops, which is corroborated by the experimental data of [1]. Proceeding from this fact, it may be concluded that direct tunneling through the potential barrier of the dielectric is not the chief mechanism of charge carrier transport in the structure. A considerable contribution to the current curve is likely to be made by the tunneling through the local levels as well.

In the present work, we also considered the distribution and mutual influence of the electric field and the form of the potential barrier of the dielectric and charge carriers in the structure and did not directly

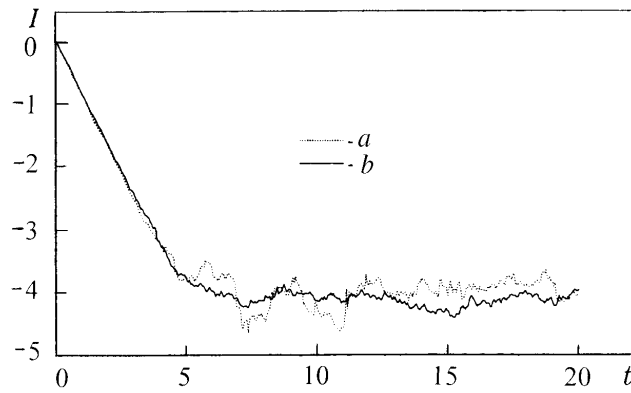


Fig. 7. Comparison of the current curves calculated on one (a) and three (b) processors under equal initial conditions. I , mA; t , 10^{-14} sec.

calculate the curvature of the contact barrier under the influence of the externally applied voltage. We constructed a grid of volt-ampere curves as a function of the height of the dielectric potential barrier (Fig. 4). The curves in Fig. 4 were calculated for the carrier pulses in the beam being injected $p_0^{\text{el}} = 3.0 \cdot 10^{-20}$ g·cm/sec and $p_0^{\text{ho}} = -1.0 \cdot 10^{-20}$ g·cm/sec. Fixing the dielectric potential barriers at the level of 0.5 eV on the assumption of an infinitesimally small hole component of current, by the constructed grids one can determine the initial pulses of electron injection from a contact at which the calculated volt-ampere curve approaches the experimental one [9]. Both curves are illustrated in Fig. 5. The dependence of the initial pulse on the external voltage (conditions on contacts) obtained for the calculated curve is given in Fig. 6. We plan to use the established relationship in the future in modeling the operation of the electron injector in the structure under investigation.

To estimate the reliability of parallel calculations, Fig. 7 presents comparison of the time dependence of current in a periodic semiconductor structure found with the aid of the parallel version of the SIMPS code with the result obtained from the sequential version. The departure of the two curves from each other was 2.7%, which demonstrates the fairly high accuracy and reliability of the paralleling model used.

Table 1 presents the results of SIMPS code tests for different numbers of processors in different configurations (count time of 20 time steps). The acceleration χ was determined as the count time on one processor t_1 divided by the count time on n_{proc} processors $t_{n_{\text{proc}}}$. The efficiency ξ was calculated as the acceleration divided by the number of processors n_{proc} . In the calculations, the execution time on one processor, the fastest one in the given configuration was used. According to Table 1, the paralleling efficiency remains fairly high for the case of two identical processors. With increasing number of processors the efficiency degrades because of the increasing number of grid accesses and amount of transferred information. The influence of the grid rate on the task paralleling efficiency can easily be determined by considering the ratio between the count time on one PII 300 MHz processor and the count time on a cluster of two PI 150 MHz processors. Initially, the performance of one PII (130.7 sec) is higher by a factor of 2.66 than of PI (347.24 sec). In the ideal case (without information transfer losses), two PI processors would carry out a test in 173.62 sec and three such processors — in 115.75 sec, i.e., two PIs would be 1.33 times slower and three PIs 1.13 times faster than one PII. In reality, with allowance made for the information exchange time in the network the efficiency of the first case would be 92.5% and of the second case 77.0%, and thus two PIs would be 1.43 times and three PIs 1.15 times slower than one PII.

The paralleling algorithm did not provide for dynamic distribution of the computational load on the processors according to their speed. Inclusion in the cluster configuration of computers differing in performance without dynamic load distribution leads to a decrease in the paralleling efficiency because of the downtime of the fast processors. Proceeding from the data obtained by us, it may be suggested that in the ideal case (with no allowance for the data transfer time and with a proportional distribution of the computational

TABLE 1. Results of the SIMPS Code Testing on a Cluster of Processors Differing in Configuration (count time of 20 time steps)

noprocs	PII 300 MHz	PII 300 MHz	PI 150 MHz	PI 150 MHz	PI 150 MHz	$t_{\text{noprocs, sec}}$	χ	$\xi, \%$
1	+					130.7		
1			+			347.24		
2	+	+				68.4	1.91	95.5
2	+		+			139.88	1.07	53.5
2			+	+		187.55	1.85	92.5
3	+	+	+			53.54	2.44	81.3
3	+		+	+		54.27	2.41	80.3
3			+	+	+	150.63	2.31	77.0
4	+	+	+	+		45.34	2.88	72.0
4	+		+	+	+	98.17	1.33	33.3
5	+	+	+	+	+	89.3	1.46	29.2

load), a cluster of two different processors (PI and PII) would run the problem in 94.96 sec. Adding to this value the data transfer time from the case of two PIs (12.93 sec), we obtain the time the PI+PII cluster needs for solving the problem with an optimum load distribution: 108.89 sec. As is seen from the table, in the experiment this time was measured to be 139.88 sec, i.e., a PII downtime of 31 sec was observed.

It should be noted that the paralleling efficiency is strongly influenced by the physical formulation of the problem and the algorithm of its solution. The problem given in the present paper is self-consistent, i.e., it requires the transfer of a large amount of data at each time step of the program, and this considerably decreases the efficiency. Another problem impeding the code paralleling turned out to be the nonequivalence of particles from the point of view of the time spent by a processor in calculating their paths. The authors were faced with a situation where "short particles" got on a slow processor and "long" ones on a fast processor. As a result, the slow processor waited for a signal from the fast one, although the number of particles on each of them was the same. The above remarks provide the possibility for further improvement of the paralleling algorithm and for increasing the count time of the problem.

Conclusions. The theoretical model constructed on the basis of the Monte Carlo method has made it possible to adequately describe the processes of charge transfer in the nc-Si/CaF₂ periodic structure. The influence of the charge carrier injection rate and the height of the potential barrier of dielectric layers on the volt-ampere characteristic of the structure has been investigated. The dependence of the contact injection rate on the external voltage has been calculated. It is noted that in all probability the direct tunneling through the potential barrier of dielectric layers is not the chief mechanism of charge carrier transport and it is necessary to additionally consider the tunneling through the local levels. The acceleration attained in the parallel version of the SIMPS code permits accurate and more realistic, in terms of time expenditures, calculations of the charge transfer characteristics in periodic structures. The paralleling technique used in the present work is also applicable to other distributed memory architectures (MPP systems).

The authors thank Prof. F. A. d'Avitaya and Candidate of Physicomathematical Sciences A. B. Filonov for supplying the materials and for steady interest in this work.

NOTATION

α_n and β_n , n -layer tri-diagonal coefficients; ϕ , electric field potential; ϵ_n , n -layer permittivity; Q_n , n -layer charge; h , grid step; r , random number in the $[0, 1]$ interval; τ , mean free time of a particle; U , exter-

nally applied potential; A , B , and C , Dresselhaus parameters; p_{0x} , p_{0y} , and p_{0z} , projections of initial pulses; x_0 , y_0 , z_0 , coordinates of the origin; E , electric field strength; e and m_{el} , electron charge and mass; $\varphi_i(x)$, image force potential; S , potential barrier width; $W(k)$ and $W(\mathcal{E})$, scattering probability of a particle; k , wave vector length of an electron or a hole; q , phonon wave vector length; Ξ_{ac} , deformation potential constant of acoustic phonons; m^* , carrier effective mass; s_{long} , longitudinal velocity of sound; \hbar , Planck constant; N_{ac} and N_{op} , number of thermodynamically equilibrium phonons; ρ , crystal density; \mathcal{E} , particle energy; k_B , Boltzmann constant; T , temperature; $\mathcal{E}_q = \hbar s_{long} q$, acoustic phonon energy; Ξ_{op} , deformation potential constant of optical phonons; ω_{op} , frequency of optical phonons. Subscripts and superscripts: n , layer number; Σ , total; i , mirror image; ac , acoustic; op , optical; $+$, for phonon absorption; $-$, for phonon emission; $*$, effective; el , electron; ho , hole; hh , "heavy" hole; $long$, longitudinal; max , maximum; min , minimum; s , sound; d , state density.

REFERENCES

1. M. Watanabe, T. Matsunuma, T. Maryuama, and Y. Maeda, *Jpn. J. Appl. Phys.*, **37**, L591–L593 (1998).
2. A. G. Nassiopoulou, F. Bassani, S. Menard, V. Tsakiri, V. Ioannou-Sougleridis, P. Photopoulos, and F. A. d'Avitaya, *J. Lumin.*, **80**, Nos. 1–4, 81–89 (1998).
3. Y. L. He, G. Y. Hu, M. B. Yu, M. Liu, J. L. Wang, and G. Y. Xu, *Phys. Rev. B*, **59**, No. 23, 15352–15357 (1999).
4. R. W. Hockney and J. W. Eastwood, *Computer Simulation Using Particles* [Russian translation], Moscow (1987).
5. A. J. Van der Steen, *Aspects of Computational Science*, NCF, The Hague (1995).
6. *OpenMP: Simple, Portable, Scalable SMP Programming*. <http://www.openmp.org/>.
7. W. Gropp, E. Lusk, and A. Skjellum, *Using MPI-Portable Parallel Programming with the Message-Passage Interface*, Cambridge, MA (1994).
8. P. S. Pacheco, *Parallel Programming with MPI*, San Francisco, CA (1997).
9. F. A. D'Avitaya, F. Bassani, I. Mihalcescu, and A. G. Nassiopoulos, in: *Physics, Chemistry, and Application of Nanostructures*, Review to NANOMEETIN'97, Singapore (1997), pp. 3–17.
10. V. M. Ivashchenko and V. V. Mitin, *Modeling of Kinetic Phenomena in Semiconductors. Monte Carlo Method* [in Russian], Kiev (1990).
11. K. C. Kao and W. Hwang, *Electron Transport in Solids* [Russian translation], Moscow (1984).
12. A. Samarskii and A. Gulin, *Numerical Methods* [in Russian], Moscow (1989).
13. V. A. Sizyuk, *Vestsi Nats. Akad. Navuk Belarusi, Ser. Fiz.-Tékh. Navuk*, No. 4, 62–66 (1997). http://www.ac.by/publications/vesti/vth97_4.html.htm.
14. A. Jelenski, I. E. Tralle, and V. A. Sizyuk, *J. Eng. Phys. Thermophys.*, **71**, No. 5, 878–885 (1998).
15. A. N. Kholod, A. B. Filonov, and V. E. Borisenko, *Dokl. Nats. Akad. Nauk Belarusi*, **41**, No. 4, 58–61 (1997). http://www.ac.by/publications/dan/dan41_4.html.
16. C. Jacoboni and L. Reggiani, *Rev. Mod. Phys.*, **55**, No. 3, 645–705 (1983).
17. L. Reggiani, P. Lugli, and V. Mitin, *Appl. Phys. Lett.*, **51**, No. 12, 295–297 (1987).
18. *MPICH for Windows NT Download Page*. <http://www-unix.mcs.anl.gov/mpi/mpich/>.